Efficiency of Blended Polyhydric Alcohols Solution on Liquefaction of Oil Palm Trunk (*Elaeis guineensis* Jacq.)

Rattana Choowang,[a,b] Jian Lin,[a,*] and Guangjie Zhao [a]

The oil palm tree is a monocotyledon, and the chemical composition varies relative to the part of its trunk. Therefore, the purpose of this study was to investigate the relationship between the chemical composition in different parts of an oil palm trunk and the rate of liquefaction. PEG#400/glycerol (4:1, w/w) was the liquefying reagent with 2% sulfuric acid as a catalyst. Liquefaction was done at the optimum conditions of liquor ratio, temperature (130 to 180 °C), and reaction time (30 to 120 min). The results revealed that the rate of liquefying was dependent on the part of the trunk. The inner zone in the top parts of the trunk had the least amount of lignin and lowest crystallinity. Thus, these parts could be liquefied faster than the other parts of the trunk. According to FTIR, XRD, and ^{13}C NMR analyses, the amorphous polymer content (comprised of lignin, hemicellulose, and disordered zones of cellulose and starch) mostly degraded at the low temperature of 140 °C for 30 min, while the crystalline regions required higher temperature (180 °C). Increasing the temperature had stronger effects than extending reaction time or the liquor ratio. Furthermore, excess in these reaction parameters caused re-condensation of the degraded liquefied products.

Keywords: Oil palm trunk; Liquefaction; Residue; Polyhydric alcohols

Contact information: a: MOE Key Laboratory of Wooden Material Science and Application, Beijing Forestry University, Beijing 100083, China; b: Faculty of Science and Industrial Technology, Prince of Songkla University, Surat Thani Campus, Mueang, Surat Thani 84000, Thailand;
** Corresponding author: linjian0702@bjfu.edu.cn*

INTRODUCTION

Oil palm trees are important agricultural crops found in Southeast Asia, especially in Indonesia, Malaysia, and Thailand. In 2017, oil palm plantations in Thailand covered a total harvested area of approximately 1.2 million hectares, representing a 55% increase from 2010. Trees are replanted in more than 24,000 hectares/year (Office of Agricultural Economics 2017) due to older trees becoming too tall and providing low yield, as well as high harvesting economic costs when the oil palm trees reach 25 years age. Therefore, more than 1 million tons of oil palm trunk biomass is created annually. Most of this biomass is left to rot in fields instead of being utilized. Regarding the chemical composition of oil palm trunks, a previous study found a high amount of carbohydrate polymers: cellulose, hemicellulose, and starch (Hashim *et al.* 2011), which are all good bio-resource materials for liquefaction to convert the material to eco-friendly products.

Liquefaction products are used in several products, such as wood adhesives, bio-plastics, activated carbon fiber, *etc*. Generally, they can be produced from lignocellulosic materials by reactions with organic polymers, phenol, and polyhydric alcohols, aided by catalysts at medium temperatures ranging from 120 °C to 180 °C (Alma *et al.* 1998; Zhang *et al.* 2006a; Pan 2011; Huang *et al.* 2015). Most prior studies have focused on phenol that

has a high ability to dissolve wood by degrading it to liquefied products (Zhang *et al.* 2006b). However, phenols are petrochemical materials and can be considered unsustainable, whereas polyhydric alcohols are low in toxicity and have low costs as liquefying reagents. Several types of polyhydric alcohols have been investigated. Yip and co-workers (2009) found that ethylene carbonate (EC) gave less residue than ethylene glycol (EG); in the case of the liquefying bamboo the process needed 5% hydrochloric acid as catalyst at 180 °C. Guo *et al.* (2014) reported that the liquefying rate of giant reed biomass was more rapid when using polyethylene glycol (PEG#400) mixed with 3% sulfuric acid at 170 °C and with a liquor ratio of 7:1 (w/w) than when using ethylene glycol solution. However, applying polyethylene glycol alone led to re-condensation during the liquefaction process and reduced yield of the product. These results match the previous report of Yamada *et al.* (2001). They demonstrated that liquefying Japanese cedar in PEG#400 solvent led to condensation after 30 min reaction time; the reaction was accelerated with 3% sulfuric acid (based on the amount of solvent) and the temperature was 150 °C. The re-condensation with excessive reaction time might be due to the condensation of lignin and 5-hydroxymethyfurfural (HMF) formed from the degraded products, and it can be retarded by adding glycerol. A mixture of PEG#400 and glycerol has been applied as an excellent liquefying reagent for various biomass types, such as corn starch, bagasse, cotton, bamboo, wheat straw, corncob, and others. Glycerol contents in the range from 10% to 20% are suitable for replacing PEG#400 liquefying reagent, based on low residue content (Yao *et al.* 1996; Hassan and Shukry 2008; Chen and Lu 2009; Zhang *et al.* 2012). Overall, the key reaction parameters are liquor ratio, catalysts, liquefaction temperature and reaction time, and these should match the structure and chemical composition of wood or other lignocellulosic raw materials (Kurimoto *et al.* 2001). Thus, the optimal liquefaction parameters must be investigated for each alternative raw material. Although the liquefaction of oil palm trunk in glycerol and ethylene glycol have been studied, the liquefaction yield was less than using the blended polyhydric alcohols (Yamada *et al.* 2001; Awalludin *et al.* 2017).

Besides, the oil palm trunk from the bottom peripheral zone of the stem can be used in furniture and in non-structural construction components (Ratnasingam and Ioras 2011). Therefore, the middle and top parts of the stem (higher than 4 meters) were considered in this research as raw materials for liquefaction products. The dependence of chemical composition in the oil palm trunk on part selected was investigated first. Reactions with PEG#400 blended with glycerol (4:1, w/w) as the liquefying agent were evaluated with varied liquor ratio, temperature and time. The catalyst was 2% sulfuric acid based on the total amount of liquefying agent. The criterion evaluated was residue content that should be minimized. Further, the wood samples were analyzed with X-ray diffraction, Fourier transform infrared (FTIR) spectroscopy, and solid state ^{13}C NMR spectroscopy.

EXPERIMENTAL

Oil Palm Trunk Raw Material

Oil palm trunks were harvested from a replantation in Surat Thani province, in Southern Thailand. The trees were felled at 60 cm from ground and cut into logs of 1 meter length. The logs that were cut from middle and top parts of the trunk were sawn into lumber with separate outer and inner zones. The lumber from different parts of trunk was cut into

chips, which were oven dried at 100 °C to reduce the moisture content. The dried chips were ground into fine powder (40- to 60-mesh) and stored in a desiccator until use.

Oil Palm Trunk Chemical Analysis

The contents of ash, Klason lignin, holocellulose, and alpha cellulose in each part of the oil palm trunk were analyzed in accordance with the Chinese standards GB/T 742 (2008), GB/T 10337 (2008), GB/T 2677.10 (1995), and GB/T 744 (1989), respectively. Measurement of each component was conducted in at least triplicate, and the results were found to be reproducible. Further, FTIR spectroscopy and X-ray diffraction were applied to assess the chemical compositions of the oil palm trunk parts.

Liquefaction Process

The mixture of PEG 400 and glycerol (4:1, w/w) as liquefaction solvent was placed in a 100 ml three-necked flask and pre-heated to desired temperature by immersion in a hot oil bath. The flask was set up with magnetic stirrer, thermometer, and reflux condenser system. Then 98% (w/w) sulfuric acid was added for 2% of the liquefaction solvent (fixed parameter in experimental design) at the target temperature and then the dried oil palm biomass with the weight ratio of 1/3, 1/4, and 1/5 were added rapidly. The target temperature was varied from 130 °C to 180 °C, and reaction time was varied from 30 min to 120 min. To end the reactions, the three-necked flask was immersed in cold water and immediately neutralized by adding 80% 1,4-dioxane (20% distilled water), modified from previous study of Yamada *et al.* (2001). The suspension was filtered with a filter paper whose oven dried weight was known, and the residue on the filter paper was dried at 103 °C until it reached a constant weight. The percentage of residue (*R*) was calculated as follows,

$$R\ (\%) = (W_r / W_o) \times 100 \quad (1)$$

where W_r is the oven-dried weight of the residue in filter cake (g) and W_o is the oven-dry weight of oil palm trunk powder (g).

Scanning Electron Microscope (SEM)

The morphology of the inner zone from the top parts of the oil palm trunk was imaged by a scanning electron microscope (Gemini SEM500, Zeiss, Oberkochen, Germany). The dried cross-section sample (2 x 2 mm) was covered with platinum layer by using a sputter rate of 0.05 nm/s for 7 min before the micrographs were taken.

Fourier Transform Infrared (FTIR) Spectroscopy

The functional groups in oil palm trunk raw material and in process residue were determined by FTIR spectrometry using the GX FT-IR system (PerkinElmer, Norwalk, CT, USA) over the scan range from 400 cm^{-1} to 4000 cm^{-1}. A 1 mg sample of residue powder was mixed with 99 mg of finely ground potassium bromide and compressed to a disk for measurement.

Solid State ^{13}C NMR Spectroscopy

Solid State ^{13}C NMR spectrometer (JNM-ECZ600R, JEOL, Tokyo, Japan) equipped with a 3.2 mm probe was used to analyze the inner zone of top parts of the trunk and its process residue. All measurements were conducted at 298 K with a MAS spinning rate of 12 kHz and relaxation time of 2 s. Each specimen was measured for 1 h.

X-ray Diffraction Analysis

The crystallinity in oil palm trunk raw material and process residue was measured by X-ray diffraction (Smart lab, Rigaku, Tokyo, Japan) equipped with Ni-filtered Cu-Kα radiation (wavelength 1.5406 nm), operated at 40 kV and 40 mA. The scans were recorded from 5° to 50° (2θ) with a scan speed of 0.5°/min and a scan step of 0.02°. The crystallinity index (*CrI*) for the residues was calculated according to the Segal method (Segal *et al.* 1959) as follows,

$$CrI = (I_{002} - I_{am}) / I_{002} \times 100 \quad (2)$$

where I_{002} is the intensity for the (002) plane and I_{am} is the intensity of the amorphous fraction.

RESULTS AND DISCUSSION

Oil Palm Trunk Chemical Analysis

Table 1 shows the ash content by zone and part of the trunk. It ranged from 2.67% to 3.78%. The outer zone in the middle part of the trunk had the highest contents of holocellulose, alpha cellulose, and acid-insoluble lignin. The chemical compositions did not greatly differ between the inner zone in the middle parts and the outer zone in the top part of the trunk. According to previous reports, oil palm trunk contains abundant starch granules, mostly in the parenchyma cells, depending on the zone and source of oil palm trunk (Tomimura 1992; Prawitwong *et al.* 2012). Therefore, the chemical composition of oil palm trunk that is indicated in Table 1 is also comprised of starch.

Table 1. Chemical Composition of the Middle and Top Parts of the Oil Palm Trunk

Chemical Composition (%)	Middle Parts		Top Parts	
	Outer zone	Inner zone	Outer zone	Inner zone
Holocellulose	54.70 (1.08)	44.60 (1.05)	44.19 (1.08)	24.08 (0.54)
α-cellulose	27.73 (0.05)	21.59 (0.29)	22.14 (0.32)	11.33 (0.58)
Acid- insoluble lignin	12.21 (0.92)	10.43 (0.79)	9.73 (0.79)	5.10 (0.32)
Ash	2.78 (0.10)	3.78 (0.08)	3.30 (0.07)	2.67 (0.05)
Note: Values in parentheses are standard deviations				

Furthermore, the FTIR spectra shown in Fig. 1A indicate that the parts of the trunk were similar with regard to functional groups of carbohydrate polymers. The α-1,4 linkages are detected at lower wavenumbers than β-1,4 linkages (Sekkal *et al.* 1995; Kizil *et al.* 2002). The outer zone of middle parts had a clear band at 1039 cm^{-1}, which indicated β-1,4 linkages of cellulose. The band consistently shifted to 995 cm^{-1} for the inner zone of the top parts, due to a higher portion of α-1,4 glycosidic linkages only found in starch. Oil palm trunk contains abundant starch granules, mostly in the parenchyma cells, depending on the zone and source of oil palm trunk (Prawitwong *et al.* 2012). This was confirmed by the XRD analysis (Fig. 1B). The X-ray diffraction pattern from the inner zone of the top part of the trunk was similar to the diffraction pattern of starch isolated from the trunk, as shown in Fig. 1B (Noor *et al.* 1999). The main crystalline peaks were observed at 2θ = 15.22°, 17.10°, 18.20°, and 22.84°. The crystalline peak at 2θ = 22.84° was less intense compared with other parts. The outer zone of the middle part of the trunk had a higher peak at 2θ =

22°, which may indicate crystalline regions in cellulose. The inner zone of the top part of the trunk had a high amount of starch, which was confirmed by the micrograph in Fig. 2. The vascular bundles (V) were surrounded by the parenchyma cells (P) that were filled with starch granules (S).

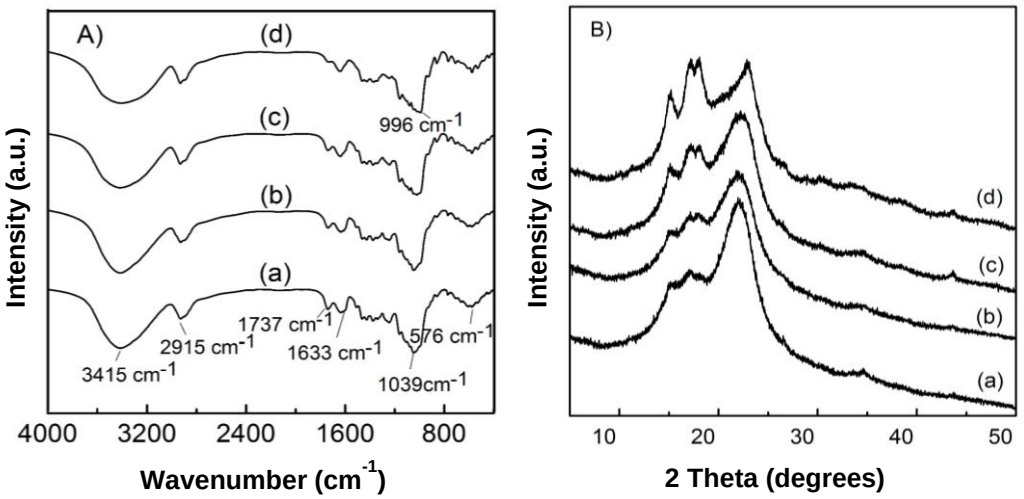

Fig. 1. FTIR spectra A) and X-ray diffraction B) of the middle parts of the trunk: outer zone (a) and inner zone (b); and top parts of the trunk: outer zone (c) and inner zone (d)

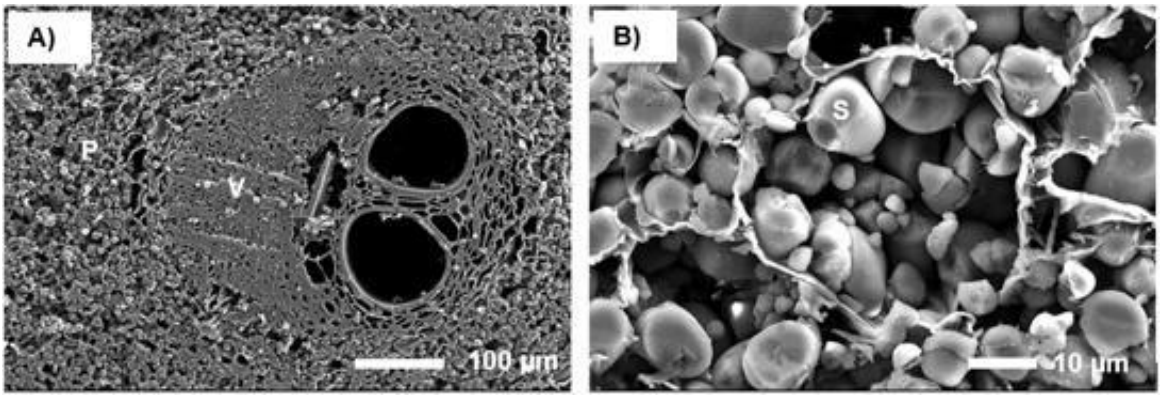

Fig. 2. Micrographs of a cross-section in the inner zone of the top parts of oil palm trunk (A) and starch granules in parenchyma cells (B) (Note: P means parenchyma cells; V means vessels; S means starch granules)

Liquefaction of Oil Palm Trunk

Influence of zone in oil palm trunk and liquor ratios

The residue was separated from the liquefaction products of different parts of oil palm trunk after the liquefaction at 140 °C for 60 min, and the residue amounts were calculated, as shown in Fig. 3. The inner zone of the top part of the trunk gave the lowest percentage of residue, while the residues amounts from the other three parts were approximately twice that of the inner zone of top part of trunk, especially for the liquor ratio of 1/3. These effects may be caused by the different amounts of chemical components in different parts of trunk. The inner zone of the top parts contained lower amounts of lignin, lower values of crystalline index, and more starch, while the other three parts

showed relative higher amount of crystalline cellulose, which is densely packed. Generally, crystalline regions need longer processing time than amorphous regions, and amorphous structures including lignin, hemicellulose, disordered zones of cellulose, and starch are easily penetrated by acidic solution and then rapidly liquefied (Hoover 2000; Zhang *et al.* 2012b).

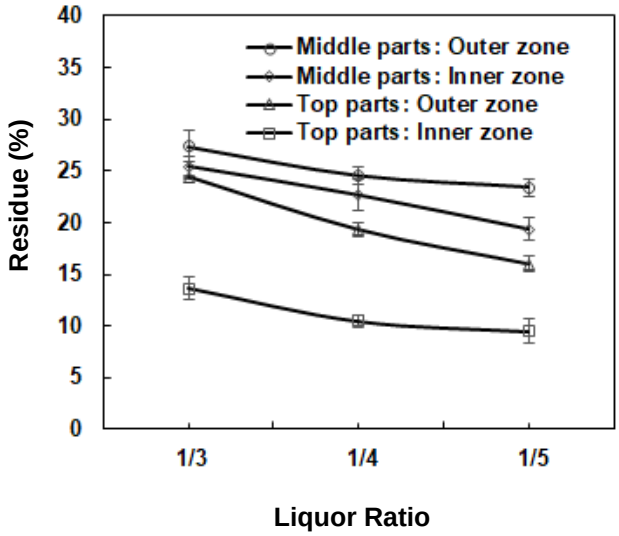

Fig. 3. The process residue (%) of oil palm trunk liquefied with PEG 400/glycerol (4:1, w/w) and 2% sulfuric acid as catalyst, at 140 °C for 60 min, with liquor ratios from 1/3 to 1/5

Liquefaction with different liquor ratios from 1/3 to 1/5 was also conducted. The resultant residue amount decreased with decreasing the liquor ratio, as shown in Fig. 3. The highest residue amounts were obtained from the liquor ratio of 1/3, while there was no significant difference in residue amounts between the ratios 1/4 and 1/5, especially for the inner zone of top part of trunk. The glycerol used with PEG 400 accelerates the liquefying reactions and inhibits re-condensation. This is because glycerol is highly polar and has a good ability to penetrate biomass and dissolve lignin. It complements the acidic breakdown of polysaccharides. Furthermore, glycerol reacts with lignin fragments, generating free radicals (Novo *et al.* 2011).

Influence of liquefaction temperature and time

Considering the fact that they had the lowest residue amount and its smaller difference in liquor ratios between 1/4 and 1/5, the inner zone of the top parts of the trunk and liquor ratio of 1/3 and 1/4 were selected for further study on the influence of liquefaction temperature and time. Figure 4 shows that the residues decreased with increasing liquefaction temperature from 130 °C to 180 °C. A strongly reduced residue with 30 min time was observed as the temperature was increased. There were small differences among the varying liquefaction times at each temperature from 140 °C to 170 °C, especially with liquor ratio 1/4. This may be caused by the rapid decomposition of most amorphous carbohydrate compounds in the inner zone of top parts of oil palm trunk such as hemicellulose and starch, which were easily transformed into small molecular under the heating and acid conditions. These results indicated that the liquefaction temperature had significantly varying effects on the residue.

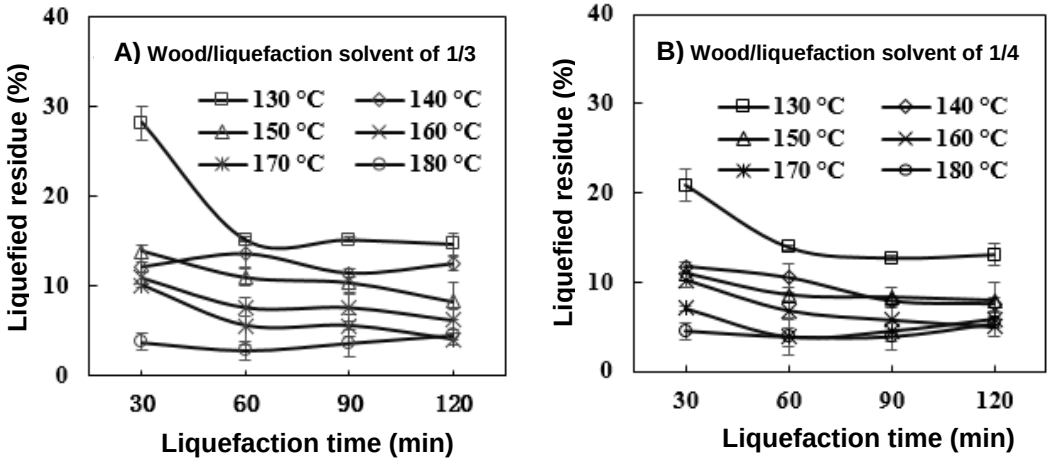

Fig. 4. The process residue (%) from the inner zone of the top parts of oil palm trunk when liquefied with PEG 400/glycerol (4:1, w/w), 2% sulfuric acid as catalyst, at 130 °C to 180 °C for various times (30 min to 120 min), with liquor ratios 1/3 (A) and 1/4 (B)

In addition, the liquefaction temperature of 140 °C gave less residue than 150 °C and became raised when the reaction time was increased from 30 min to 60 min, but this situation was not evident with the liquor ratio of 1/4 (Fig. 4B). This was due to the rapid degradation of oil palm component in an acidic liquefaction solution, leading to a high concentration of sugars. In particular, glucose and xylose, which are the main sugars in oil palm, including the intermediate chemicals derived from sugars, were transformed to levulinic acids such as HMF and furfural. Sugars and furan products can be condensed among themselves and decomposed again, depending on the temperature, time, and acidity of the solvent (Hoover 2000; Kobayashi *et al*. 2004; Sarwono *et al*. 2017; Filiciottoa *et al*. 2018). However, Fig. 4 shows that the residue amounts increased after 60 min reaction time in the case of only 180 °C for the liquor ratio of 1/3 and both 170 °C and 180 °C for the liquor ratio of 1/4, due to the re-condensation of lignin and 5-hydroxymethylfurfural (HMF) products from glucose at relatively higher temperature (Yamada *et al.* 2001). In addition, high temperatures and prolonged reaction times promote the polymerization and/or curing of liquefied products (Ugovšek and Sernek 2013; Kim *et al.* 2016).

Characterization of Resultant Residue

FTIR analysis

FTIR is an extremely useful method to investigate the functional groups of polymers. Figure 5(A) shows the FTIR spectra of oil palm trunk, and its residue after liquefaction at various temperatures for 30 min. In the spectrum of oil palm, the band centered at 3410 cm^{-1} was assigned to the stretching vibrations of hydroxyl groups, mainly in the carbohydrate polymers such as starch, hemicellulose, and cellulose, as the lignin content is only about 5.1% in oil palm trunk. After liquefaction, the broad peak had transformed into a sharp one, and the band shifted to the higher wavenumber 3431 cm^{-1} in all the residues after liquefaction, indicating the decomposition of starch and cleavage of hydrogen bonds. As the liquefaction temperatures increased, the skeletal mode vibrations of the pyranose ring at wavenumber 576 cm^{-1} and the C-H stretching vibrations at 2930 cm^{-1} slightly decreased, which due to the decomposition of amorphous starch. When the liquefaction temperature was 180 °C, the peak at 576 cm^{-1} almost disappeared. This may

indicate the decomposition of all amorphous carbohydrate polymers and most of the cellulose, leading to the low 3.7% residue content.

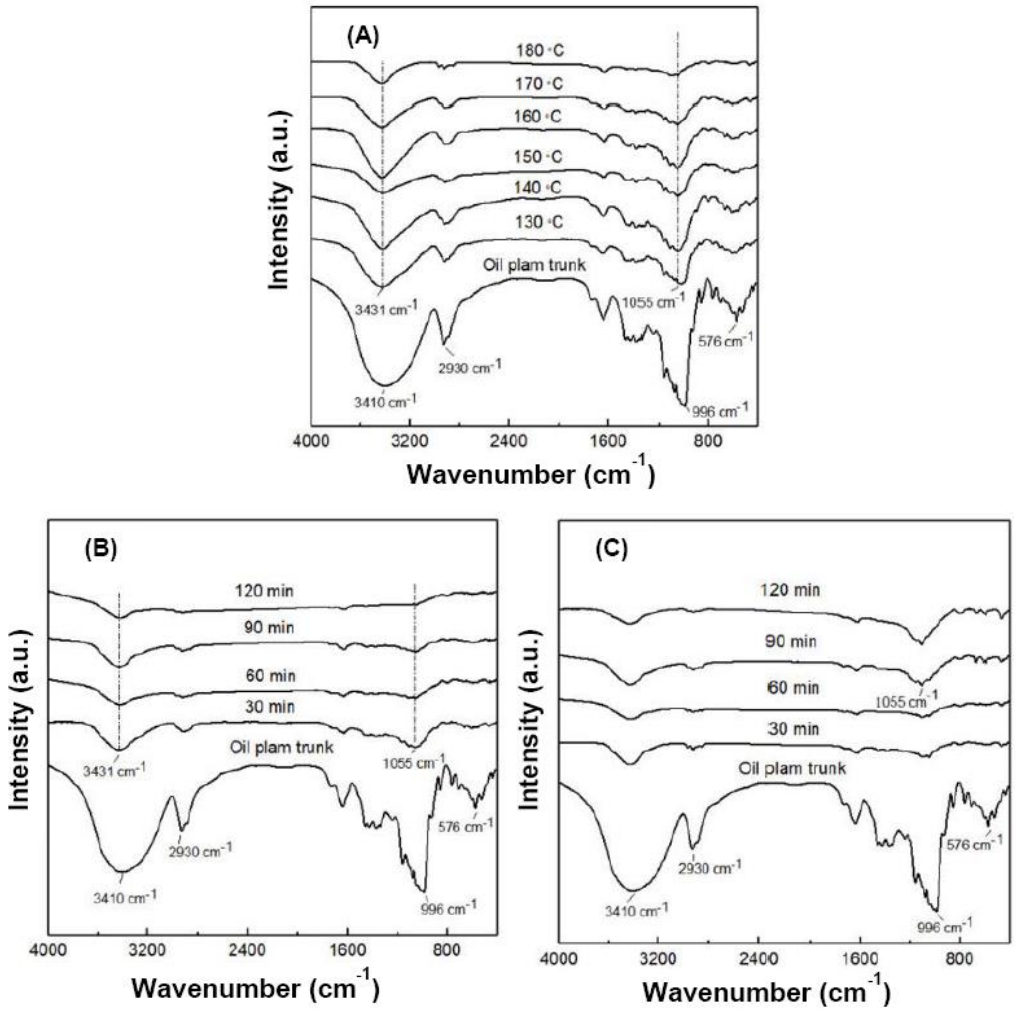

Fig. 5. FTIR spectra of the oil palm trunk and its residue liquefied with liquor ratio 1/3 at the different temperatures for 30 min (A), and with the different reaction times at 170 °C (B) and 180 °C (C)

The FTIR spectra of residues after liquefaction for various times at 170 °C are shown in Fig. 5(B). Compared with the raw material, the residue from liquefaction for 30 min exhibited a relatively sharp peak at 3431 cm^{-1} from the decomposition of starch. The peak at 1055 cm^{-1} represents ether bonds becoming weaker up to 60 min of liquefaction, which can be attributed to the decomposition of non-crystalline cellulose, accompanied by a decrease in residue from 10.1% to 5.6%. With prolonged liquefaction for 120 min, all peaks became weak from the loss of crystalline regions in cellulose. The peaks at 576 cm^{-1} and 2930 cm^{-1} also became gradually weaker. However, the residue after liquefaction at 180 °C is presented in Fig. 5(C). Almost all chemical components were decomposed with 60 min of liquefaction, which is quicker than at 170 °C. The peak at 1055 cm^{-1} was obvious after 60 min, and caused by the polymerization of liquefied products at a higher temperature and the formation of residue. Thus, the residue content increased from 60 min to 120 min of liquefaction.

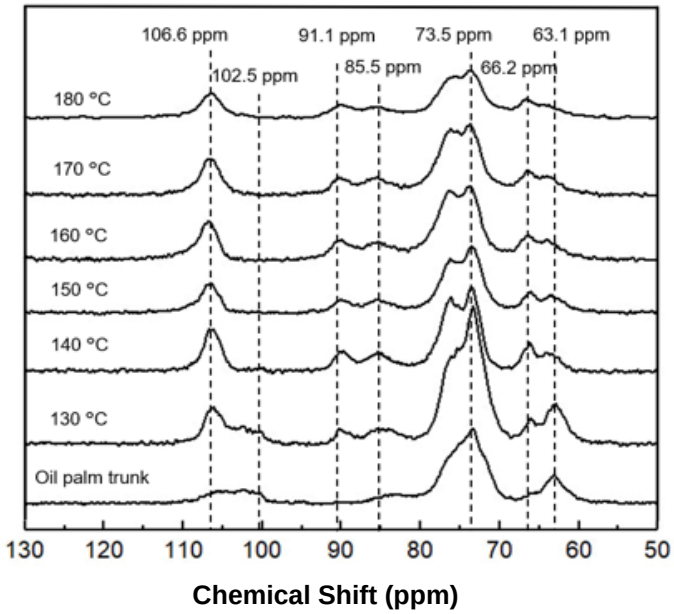

Fig. 6. Solid state ^{13}C NMR spectroscopy of oil palm trunk and its residue from liquefaction at 130 °C, 140 °C, 150 °C, 160 °C, 170 °C and 180 °C for 30 min

Solid state ^{13}C NMR spectroscopy

The solid-state ^{13}C NMR spectra of oil palm trunk and its residues from different liquefaction temperatures for 30 min are shown in Fig. 6. For the oil palm raw material, the main peak at 73.5 is related to C2, C3, and C5 carbons in the pyranose ring. The signals at 63.1 ppm and 85.5 ppm demonstrate C6 and C4 carbons in non-crystalline regions, respectively, while signals in the range from 102.5 ppm to 106.6 ppm are attributed to C1 reflect a combination of α and β C1 carbons in starch and cellulose, respectively (Wi *et al.* 2015). The C6 carbon in crystalline cellulose can usually be detected at 66.2 ppm, but the peak for oil palm raw material is very weak. However, this peak can be clearly seen after liquefaction at 140 °C. Similarly, the C1 carbon of crystalline regions was observed at 106.6 ppm because of loss of α form of C1 carbon in starch (102.5 ppm), which gives lower position of signal than the β form of cellulose (Chen *et al.* 2005). The C4 carbon of crystalline region that was detected at 90.1 ppm appeared clearly after liquefaction. In contrast, the C6 carbon of the non-crystalline region ($-CH_2OH$) at 63.1 had continuously decreasing signal when the liquefaction temperature increased from 130 to 180 °C. The signals that indicate the crystalline region were at 66.2 ppm (C6), 90.1 (C4) ppm, and 106.6 ppm (C1), and remained weak with 180 °C for 30 min treatment. Therefore, most amorphous carbohydrates (hemicellulose and starch as well as amorphous regions of cellulose) were degraded by liquefaction at 140 °C for 30 min. The crystalline regions were mostly destroyed the higher 180 °C temperature by 30 min reaction time, a fact also confirmed by the XRD analysis.

XRD analysis

The chemical components in oil palm trunk were liquefied at various temperatures because of their different crystallinities, with crystalline structures remaining in the residues. The X-ray diffractograms of oil palm trunk and residues obtained by processing

at 130 °C to 180 °C for 30 min are presented in Fig. 7 (A). For oil palm the typical peaks at 2θ values 15.2 ° and 22.8 ° are attributed to the (110) and (002) crystallographic planes, respectively, indicate the crystalline structures in cellulose I. When increasing reaction temperature from 130 °C to 170 °C, the peaks at 2θ = 22.8 ° became narrower and sharper, indicating relative increase of intensities for the (002) crystallographic plane. The corresponding crystallinity indexes were 51.7%, 74.0%, 73.0%, 75.5%, and 78.4%, respectively, much higher than the 21.1% of oil palm. This may be due to the selective decomposition amorphous structures, especially in amylose. Furthermore, the conversation of the amorphous zones to crystalline can occur (Atichokudomchai *et al.* 2001; Wang *et al.* 2014). Much of the crystalline regions were destroyed within 30 min at 180 °C according to the peak at (002) (2θ = 22.8°) with relatively low intensity. The degradation of crystalline regions was promoted by the organic acids such as acetic acid, formic acid, and levulinic acid, from the degradation of chemical components during liquefaction at a high temperature (Yamada and Ono 2001; Rezzoug and Capart 2002). The one sharp and strong peak at 2θ around 25.4° was accompanied by other smaller peaks at higher 2θ obvious in the X-ray diffractogram of residue from liquefaction at 180 °C. These peaks are related to crystalline silica, which is the main component in ash from oil palm trunks (Saka *et al.* 2008).

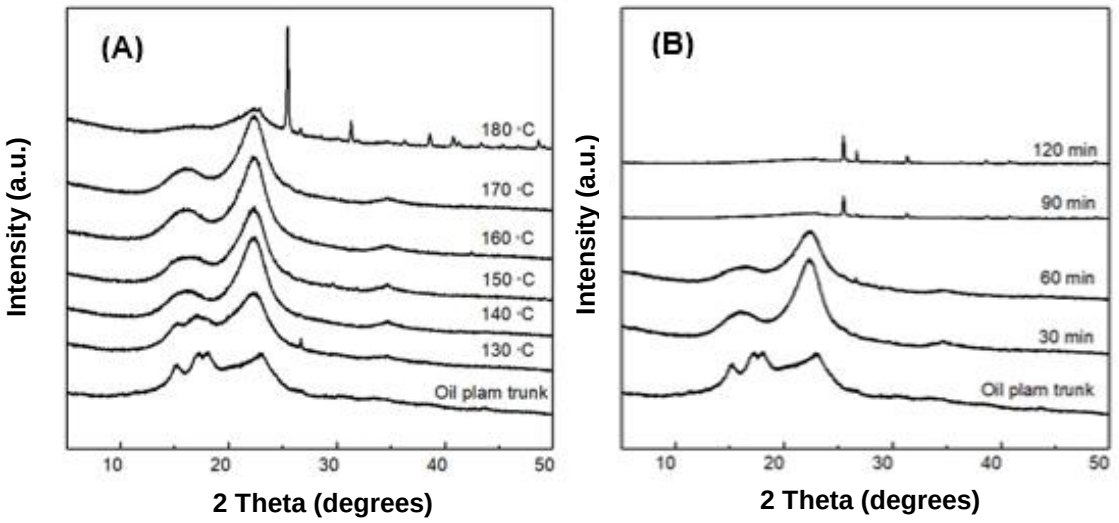

Fig. 7. X-ray diffraction patterns of the oil palm trunk and its residue after liquefaction by using the liquor ratio of 1/3 at different temperatures for 30 min (A), and different reaction times at 170 °C (B)

The X-ray diffractograms of residue from the liquefaction for different times from 30 min to 120 min at 170 °C are presented in Fig. 7 (B). Compared with the oil palm, the residues exhibited completely different patterns. When the liquefaction time increased, the peak at 2θ = 22.8° first became sharper and then gradually smaller because of the decomposition of cellulose, leading to a decrease in crystallinity index from 78.4% to 35.7%. Weaker and broader peaks were obvious after liquefaction for 90 min. The peak at 2θ = 15.2° gradually weakened and disappeared after 90 min and 120 min, indicating that the crystalline regions in cellulose were almost destroyed. These results agree well with the earlier discussed FITR and NMR results.

CONCLUSIONS

1. The oil palm trunk consists mainly of carbohydrate polymers, and especially the inner zone of the top part is rich in starch, which is suitable for use as raw material for liquefaction.
2. The residue amount of liquefaction is reduced with decreasing the liquor ratio and increasing the liquefaction temperature. Within the initial 30 min of liquefaction, the degradation of most amorphous carbohydrates, such as hemicellulose and starch as well as amorphous regions of cellulose, was completed even at the low 140 °C temperature. By contrast, the crystalline regions were mostly destroyed at the higher 180 °C temperature. The residue amount increased after 60 min of liquefaction at 180 °C, mainly due to the re-condensation of liquefied products.
3. Based on the least amount of residue, the liquor ratio of 1/3, liquefaction temperature of 180 °C, and reaction time of 30 min are recommended as the optimized condition of the inner zone of top parts of oil palm trunk with PEG 400/glycerol (4:1, w/w) under 2% sulfuric acid as a catalyst.

ACKNOWLEDGMENTS

The authors are grateful for the support of "The Fundamental Research Funds for the Central Universities" (Grant No. 2018ZY02).

REFERENCES CITED

Atichokudomchai, N., Shobsngob, S., Chinochoti, P., and Varavinit, S. (2001). "A study of some physicochemical properties of high-crystalline tapioca starch," *Starch/Stärke* 53, 577-581. DOI: 10.1002/1521-379X(200111)53:11<577::AID-STAR577>3.0.CO;2-0

Alma, M. H., Yoshioka, M., Yao, Y., and Shiraishi, N. (1998). "Preparation of sulfuric acid-catalyzed phenolated wood resin," *Wood Sci. Technol*. 32, 297-308. DOI: 10.1007/BF00702897

Awalludin, M. F, Sulaiman, O., Hashim, R., and Yhaya, M. F. (2017). "Assessment of oil palm trunk liquefaction in glycerol and ethylene glycol by 24-1 fraction factorial design," *J. Jpn. Inst. Energy* 98, 319-325. DOI: 10.3775/jie.96.319

Chen, F., and Lu, Z. (2009). "Liquefaction of wheat straw and preparation of rigid polyurethane foam from the liquefaction products," *J. Appl. Polym. Sci*. 111, 508-516. DOI: 10.1002/app.29107

Chen, Y. Y., Luo, S. Y., Hung, S. C., Chan, S. I., and Tzou, D. L. M. (2005). "^{13}C Solid-state NMR chemical shift anisotropy analysis of the anomeric carbon in carbohydrates," *Carbohydr. Res*. 340, 723-729. DOI: 10.1016/j.carres.2005.01.018

Filiciottoa, L., Balu, A. M., van der Waal, J. C. and Luque, R. (2018). "Catalytic insights into the production of biomass-derived side products methyl levulinate, furfural and humins," *Catal. Today* 302, 2-15. DOI: 10.1016/j.cattod.2017.03.008

GB/T 744 (1989). "Pulps – Determination of α-cellulose," Standardization Administration of China, Beijing, China.

GB/T 2677.10 (1995). "Fibrous material – Determination of holocellulose," Standardization Administration of China, Beijing, China.

GB/T 742 (2008). "Fibrous raw material, pulp, paper and board – Determination ash," Standardization Administration of China, Beijing, China.

GB/T 10337 (2008). "Pulps-determination of alcohol-benzene solubles," Standardization Administration of China, Beijing, China.

Guo, Z. H., Liu, Y. N., Wang, F. Y., and Xiao, X. Y. (2014). "Liquefaction of metal-contaminated giant reed biomass in acidified ethylene glycol system: Batch experiments," *J. Cent. South Univ*. 21, 1756-1762. DOI: 10.1007/s11771-014-2121-2

Hashim, R., Nadhari, W. N. A. W., Sulaiman, O., Kawamura, F., Hiziroglu, S., Sato, M., Sugimoto, T., Seng, T. G., and Tanaka, R. (2011). "Characterization of raw materials and manufactured binderless particleboard from oil palm biomass," *Mater. Design* 32, 246-254. DOI: 10.1016/j.matdes.2010.05.059

Hassan, E.-b.M., and Shukry, N. (2008). "Polyhydric alcohol liquefaction of some lignocellulose agricultural residue," *Ind. Crop. Prod*. 27, 33-38. DOI: 10.1016/j.indcrop.2007.07.004

Hoover, R. (2000). "Acid-treated starches," *Food Rev. Int*. 16(3), 369-392. DOI: 10.1081/FRI-10010029

Huang, Y., Ma, E., and Zhao, G. (2015). "Thermal and structure analysis on reaction mechanisms during the preparation of activated carbon fibers by KOH activation from liquefied wood based fibers," *Ind. Crop. Prod*. 69, 447-455. DOI: 10.1016/j.indcrop.2015.03.002

Kim, K. H., Yu, J. H., and Lee, E. Y. (2016). "Crude-glycerol mediated liquefaction of saccharification residues of sunflower stalks for production of lignin bioplyols," *J. Ind. Eng. Chem*. 38, 175-180. DOI: 10.1016/j.jiec.2016.05.002

Kizil, R., Irudayaraj, J., and Seetharaman, K. (2002). "Characterization of irradiated starches by using FT-Raman and FTIR spectroscopy," *Agric. Food Chem*. 50(14), 3912-3918. DOI: 10.1021/jf011652p

Kobayashi, M., Asano, T., Kajiyama, M., and Tomita, B. (2004). "Analysis on residue formation during wood liquefaction with polyhydric alcohol," *J. Wood. Sci*. 50(5), 407-414. DOI: 10.1007/s10086-003-0596-9

Kurimoto, Y., Koizumi, A., Doi S., Tamura, Y., and Ono, H. (2001). "Wood species effects on the characteristics of liquefied wood and the properties of polyurethane prepared from the liquefied wood," *Biomass Bioenergy* 21(5), 381-390. DOI: 10.1016/S0961-9534(01)00041-1

Noor, M. A. M, Mohd, A. M. D., Islam, Md. N., and Mehat, N. A. (1999). "Physico-chemical properties of oil palm trunk starch," *Starch/Stärke* 51, 293-301. DOI: 10.1002/(SICI)1521-379X(199909)51:8/9<293::AID-STAR293>3.0.CO;2-F

Novo, L. P., Gurgel, L. V. A., Marabezi, K., and Curvelo, A. A. D. S. (2011). "Delignification of sugarcane bagasse using glycerol-water mixtures to produce pulps for saccharification," *Bioresource Technol*. 102, 10040-10046. DOI: 10.1016/j.biortech.2011.08.050

Office of Agricultural Economics (2017). "Agricultural statistics of Thailand 2016," Bangkok, Thailand. p. 35.

Pan, H. (2011). "Synthesis of polymers from organic solvent liquefied biomass: A review," *Renew. Sust. Energ. Rev*. 15, 3454-3463. DOI: 10.1016/j.rser.2011.05.002

Prawitwong, P., Kosugi, A., Arai, T., Deng, L., Lee, K.C., Ibrahim, D., Murata, Y., Sulaiman, O., Hashim, R., Sudesh, K., Ibrahim, W.A., Saito, M., and Mori, Y. (2012).

"Efficient ethanol production from separated parenchyma and vascular bundle of oil palm trunk," *Bioresource Technol*. 125, 37-42. DOI: 10.1016/j.biortech.2012.08.136

Ratnasingam, J., and Ioras, F. (2011). "Fatigue strength and design stress of oil palm wood for furniture application," *Eur. J. Wood. Prod*. 69, 507-509. DOI: 10.1007/s00107-010-0476-0

Rezzoug, S. A., and Capart, R. (2002). "Liquefaction of wood in two successive steps: solvolysis in ethylene-glycol and catalytic hydrotreatment," *Applied Energy* 27, 631-644. DOI: 10.1016/S0306-2619(02)00054-5

Saka, S., Munusamy, M. V., Shibata, M., Tono, Y., and Miyafuji, H. (2008). "Chemical constituents of the different anatomical parts of the oil palm (*Elaeis guineensis*) for their sustainable utilization," in: Seminar Proceedings, Natural Resources and Energy Environment, Kyoto, Japan, pp. 19-34.

Sarwono, A., Man, Z., Muhammad, N., Khan, A. S., Hamzah, W. S. W., Rahim, A. H. A., Ullah, Z., and Wilfred, C. D. (2017). "A new approach of probe sonication assisted ionic liquid conversion of glucose, cellulose and biomass into 5 hydroxymethyfurfural," *Utrason. Sonochem*. 37, 310-319. DOI: 10.1016/j.ultsonch.2017.01.028

Segal, L., Creely, J. J., Martin Jr., A. E., and Conrad, C. M. (1959). "An empirical method for estimating the degree of crystallinity of native cellulose using the X-Ray diffractometer," *Text. Res. J*. 29, 786-794. DOI: 10.1177/004051755902901003

Sekkal, M., Dincq, V., Legrand, P., and Huvenne, J. P. (1995). "Investigation of the glycosidic linkages in several oligosaccharides using FT-IR and FT Raman spectroscopy," *J. Mol. Struct*. 349, 349-352. DOI: 10.1016/0022-2860(95)08781-P

Tomimura, Y. (1992). "Chemical characteristics of oil palm trunk," *Bulletin of the Forestry and Forest Products Research Institute* 362, 133-42.

Ugovšek, A., and Sernek, M. (2013). "Characterization of the curing of liquefied wood by rheometry, DEA and DSC," *Wood Sci. Technol*. 47, 1099-1111. DOI: 10.1007/s00226-013-0565-4

Wang, Q., Chen, Q., Qiao, Q., and Sugiyama, K. (2014). "Process analysis of the waste bamboo by using polyethylene glycol solvent liquefaction," *Int. J. Sus. Dev. Plann*. 9(5), 647-657. DOI: 10.2495/SDP-V9-N5-647-657

Wi, S. G., Cho, E. J., Lee, D. S., Lee, S. J., Lee, Y. J., and Bae, H. J. (2015). "Lignocellulose conversion for biofuel: A new pretreatment greatly improves downstream biocatalytic hydrolysis of various lignocellulosic materials," *Biotechnol. Biofuels* 8 (228), 1-11. DOI: 10.1186/s13068-015-0419-4

Yamada, T., Hu, Y., and Ono, H. (2001). "Condensation reaction of degraded lignocellulose during wood liquefaction in the presence of polyhydric alcohols," *J. Adh. Socy. Japan*. 37(12), 471-478. DOI: 10.11618/adhesion.37.471

Yamada, T., and Ono, H. (2001). "Characterization of the products resulting from ethylene glycol liquefaction of cellulose," *J. Wood Sci*. 47, 458-464. DOI: 10.1007/BF00767898

Yao, Y., Yoshioka, M., and Shiraishi, N. (1996). "Water-absorbing polyurethane foams from liquefied starch," *J. Appl. Polym. Sci*. 60, 1939-1949. DOI: 10.1002/(SICI)1097-4628(19960613)60:11<1939::AID-APP18>3.0.CO;2-W

Yip, J., Chen, M., Szeto, Y. S., and Yan, S. (2009). "Comparative study of liquefaction process and liquefied product from bamboo using different organic solvents," *Bioresource Technol*. 100, 6674-6678. DOI: 10.1016/j.biortech.2009.07.045

Zhang, H., Ding, F., Luo, C., Xiong, L., and Chen, X. (2012a). "Liquefaction and characterization of acid hydrolysis residue of corncob in polyhydric alcohols," *Ind. Crop. Prod*. 39, 47-51. DOI: 10.1016/j.indcrop.2012.02.010

Zhang, H., Pang, H., Shi, J., Fu, T., and Liao, B. (2012b). "Investigation of liquefied wood residues based on cellulose, hemicellulose, and lignin," *J. Appl. Polym. Sci*. 123, 850-856. DOI: 10.1002/app.34521

Zhang, Y., Ikeda, A., Hori, N., Takemura, A., One, H., and Yamada, T. (2006a). "Characterization of liquefied product from cellulose with phenol in the presence of sulfuric acid," *Bioresource Technol*. 97, 313-321. DOI: 10.1016/j.biortech.2005.02.019

Zhang, Q., Zhao, G., and Chen, J. (2006b). "Effect of inorganic acid catalysts on liquefaction of wood in phenol," *Front. For. China*. 2, 214-218. DOI: 10.1007/s 11461-006-0002-z

Article submitted: December 2, 2018; Peer review completed: January 19, 2019; Revised version received: February 1, 2019; Accepted: February 7, 2019; Published: February 15, 2019.
DOI: 10.15376/biores.14.2.2759-2772